IEEE Photonics Journal
An IEEE Photonics Society Publication

Open Access

Metal Oxide-Graphene-Based Quasi-D-Shaped Optical Fiber Plasmonic Biosensor

Volume 9, Number 4, August 2017

Guowen An
Shuguang Li
Haiyang Wang
Xuenan Zhang

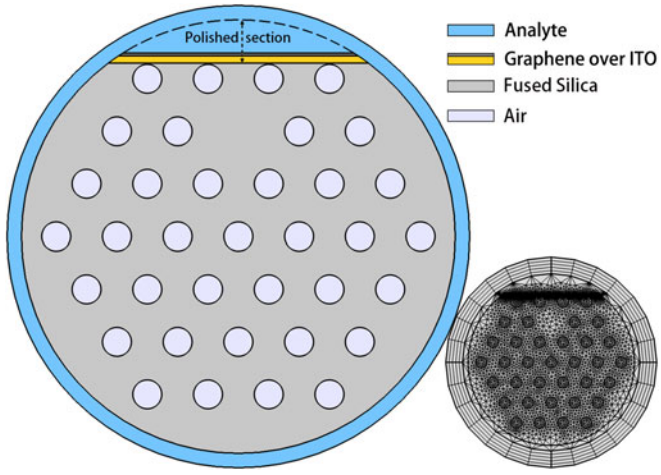

DOI: 10.1109/JPHOT.2017.2722543
1943-0655

IEEE photonics SOCIETY

IEEE

Metal Oxide-Graphene-Based Quasi-D-Shaped Optical Fiber Plasmonic Biosensor

Guowen An, Shuguang Li, Haiyang Wang, and Xuenan Zhang

College of Information Science and Engineering, Northeastern University, Shenyang 110819, China

DOI:10.1109/JPHOT.2017.2722543

Manuscript received May 23, 2017; revised June 16, 2017; accepted June 28, 2017. Date of publication July 5, 2017; date of current version July 17, 2017. This work was supported in part by the Natural Science Foundation of Liaoning Province, China under Grant 2014020020, in part by the Fundamental Research Funds for the Central Universities under Grants N130404001 and N150403003, and in part by the Project-sponsored by SRF for ROCS, SEM (47-6). Corresponding author: Shuguang Li (e-mail: lishuguang@ise.neu.edu.cn).

Abstract: A quasi-D-Shaped photonic crystal fiber plasmonic biosensor operating in near infrared is proposed for refractive index sensing. Chemically stable graphene and indium tin oxide layers are used outside the fiber structure to realize a simple detection mechanism. The design of quasi-D-shaped fiber makes the sensor configuration more simple and easy to use. And the proposed sensor shows the wavelength interrogation sensitivity of 3908–10693 nm/RIU in the dynamic index range from 1.33 to 1.38. It also shows the maximum amplitude sensitivity of 95 RIU^{-1} at the wavelength of 2040 nm with the analyte refractive index (RI) of 1.37. Compared with traditional D-shaped optical fiber, the proposed quasi-D-Shaped fiber has the advantages of easier to make and the promising results makes it a potential candidate for detecting biomolecules, water quality analysis and other analytes.

Index Terms: Photonic crystal fibers, surface plasmons, sensors, surface plasmon resonance.

1. Introduction

The surface plasmon excited by light is called Surface plasmon resonance(SPR) [1] of localized surface plasmon resonance(LSPR) or nano size metal structure [2]. And this effect has been more and more used in the sensors which have extensive applications in the area of water quality analysis, clinical medicine detection, and pharmaceutical testing (liquid medicine) [3]–[5]. The photonic crystal fiber(PCF) is used as the carrier of SPR sensing has become very popular in the past decade [6], [7] due to its unique excellent performance relative to the traditional fiber [8], [9]. However, among the numerous SPR-based PCF sensors, many sensors are not very convenient to use due to its unreasonable detection structure or unsatisfactory sensitivity such as filled the analytes in the air holes of PCF [10], [11], complex structure that makes the manufacturing process difficult [12] [13], ultra low sensitivity [14], filled the air hole with superfine metal wire [15] and the flat-fiber structure that difficult to weld with fiber [16]. One can not help thinking how to fill the analytes into the air hole quickly in the process of real-time detection of the samples?

Thus, in order to solve this kind of problem and make operation more convenient, more and more D-shaped PCF sensors have emerged [17]–[19]. Benefits from its natural shape advantage, the metal film which is used as the sensing medium can be easily plated on the flat surface which is side polished [20]. And naturally the real-time detection can be realized with the analytes be placed on the outside of the fiber [21]. However, to our knowledge, most of the D-shaped PCF sensors cut almost half of the fiber or in other words with a deep polishing depth [22]–[24]. Thus, it creates difficulties for manufacturing. Because the deeper the depth of polishing, the greater the likelihood of damage to the fiber and the polished surface will become uneven if one polish into the air hole layer [22]. If the polishing platform is not smooth, it will affect the smoothness of the metal film and then affect the sensing performance [25].

In this paper, in order to solve the above problems and by combining the advantages of D-shaped fiber, we propose and numerically investigate a quasi-D-shaped photonic crystal fiber (PCF) SPR sensor with a ultra short polishing depth. The production process will be very simple by placing the core on the edge of the cladding. In this way, we only need to polish off a small portion of the fiber and a same or even better sensing performance can be achieved compared with the previously mentioned sensors at the same time. And such treatment can also make up the defect of easier to break caused by large polished part.

2. Structure and Theoretical Modelling

Finite element method (FEM) is used by considering perfectly matched layer (PML) boundary conditions of the mapped type as a radiation absorber to analyze the guiding properties of the proposed sensor. A conducting metal oxide (CMO) of indiumtin oxide (ITO) whose properties have been found to be such that tunable plasma frequency [26] and high optical transparency in visible to near infrared (IR) region [27] was used as the sensing medium. The variation in real and imaginary parts of the permittivity of ITO is computed by using the relation [28]:

$$\varepsilon_m(\lambda) = \varepsilon_\infty - \frac{\lambda^2 \lambda_c}{\lambda_p^2(\lambda_c + i\lambda)} \tag{1}$$

where ε_∞ is the dielectric constant for the infinite value of the frequency. $\lambda_p = 5.649710^7$ m and $\lambda_c = 11.2107610^6$ m are the plasma and collision wavelengths of ITO respectively.

Graphene is used to be deposited over ITO in order to raise the performance of sensors due to the $\pi - \pi$ stacking. Besides, the high surface to volume ratio and superior plasmonic properties of graphene can also increase the absorption of analyte molecules which is very suitable for improving the sensing performance [29]–[31]. The complex RI of graphene can be obtained from the equation [32] $n_g = 3 + \frac{iC_1\lambda}{3}$, where constant $C_1 \approx 5.446\,\mu\text{m}^{-1}$ and λ is the vacuum wavelength in μm. Besides, the thickness of the graphene layer can be calculated as $t_g = 0.34\,\text{nm} \times L$, where L is the number of graphene layers.

Fig. 1 is a magnified diagram where analyte will flow through the sensing medium. ITO coated with graphene is deposited on the polished plane of the quasi-D-shaped PCF. In order to reduce computing time and memory, a complete mesh composed of 319680 domain elements and 18387 boundary domain elements is constructed by using commercial software known as COMSOL.

With regard to fabrication, as we moved the core to the edge of the fiber, the polishing process will become easier because the parts that require polishing will be greatly reduced compared with other common D-shaped sensors [18], [26], [33]. And such design can also help to enhance the impact toughness of the optical fiber. The thin film of ITO can be prepared by various methods such as chemical vapor deposition [34], pulsed laser deposition [35], and dc magnetron sputtering [36]. After a series of operations such as cleaning, drying, UV curing, etc. the graphene can also be deposited on the ITO [37].

The experimental setup for analysing the RI of the analytes is shown in Fig. 2. A wide-band light source may use to lunch into the quasi-D-shaped PCF and the evanescent field can easily penetrate the metal film, then a strong mode coupling occurs between the core and spp mode. The

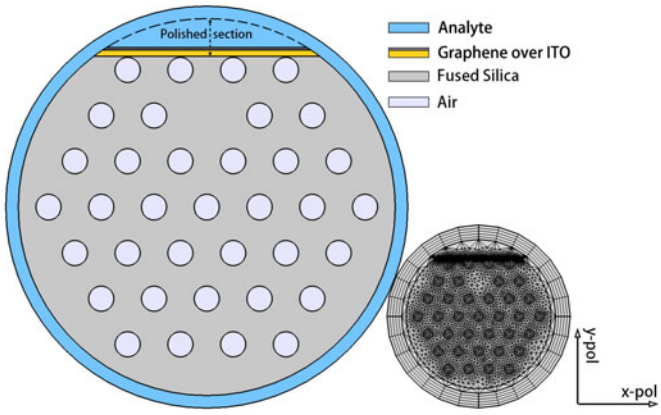

Fig. 1. Cross sectional view of the proposed structure.

Fig. 2. Schematic diagram of the proposed sensor set-up.

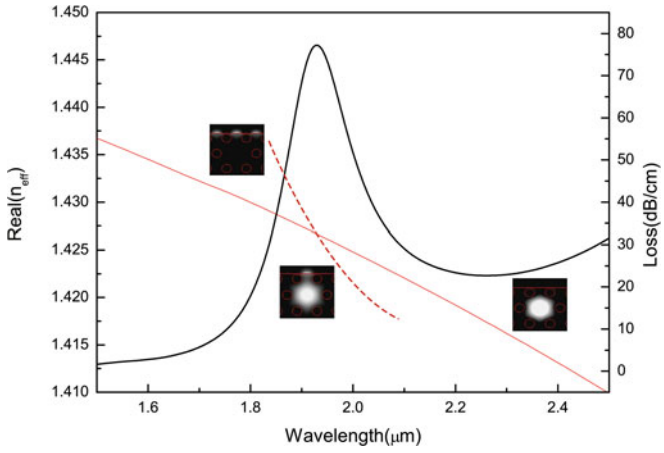

Fig. 3. Dispersion relations of core guided mode and plasmonic mode(the red dashed and solid lines) and loss spectra(black solid line) with the RI of the analyte $n = 1.36$.

analyte sample flowing surround the optical fiber with different RI can change the phase matching condition by evanescent field and then result in a blue or red shift of the loss peak which can be easily detected by an optical spectrum analyzer (OSA).

3. Result and Discussion

3.1. Investigation of the Quasi-D-Shaped PCF SPR Sensor Performance

Fig. 3 shows the loss spectra(black) and the dispersion relations of fundamental mode and SPP mode (red) with the thickness of ITO film $t_I = 100$ nm and a monolayer of graphene whose thickness is 0.34 nm($L = 1$). Unless otherwise specified, $t_I = 100$ nm and $L = 1$ are considered for all simulations. When the real n_{eff} of the core guided mode is equal to the SPP mode, resonant coupling between the two modes occur and the loss increased sharply which can be calculated

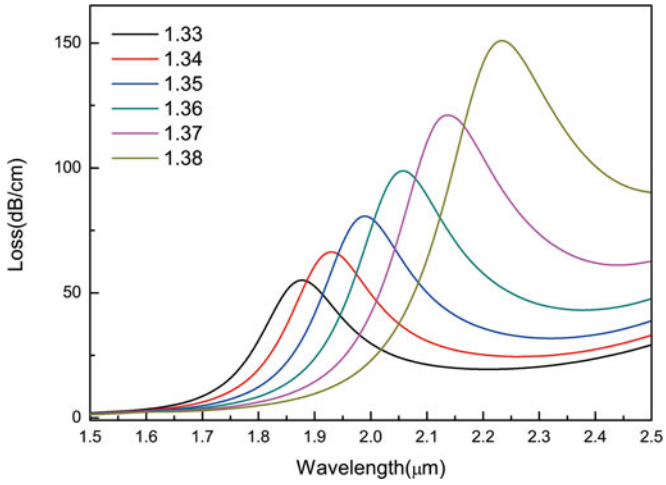

Fig. 4. Variation of loss with refractive index of analyte.

from $\alpha_{loss} = 8.686 \times \frac{2\pi}{\lambda} \mathrm{Im}(n_{\mathrm{eff}})$, where λ is in micron scale. It is generally known that the plasmionc mode is very sensitive to the change in the RI of the dielectric surface and therefore any tiny changes of the refractive index of the analytes could cause great changes of the surface plasmon resonance(SPR) points.

To study the sensor performance, we take aqueous analyte as an example with the dynamic index range from 1.33 to 1.38. As can be seen in Fig. 4 that with the refractive indexes of the analyte ranging from $n_a = 1.33$ to $n_a = 1.38$, the resonance peak experiences a red shift and the peak value also increased. The maximum shifting occurs during $n_a = 1.37$ to $n_a = 1.38$ is mainly because that with the increase of the coupling wavelength, the ability of PCF to limit light will be significantly weakened, and then more evanescent waves will interact with the external analyte. That is to say, the sensitivity of the sensor will increase. The reason why we set the detection upper limit to $n_a = 1.38$ is that when n_a continues to increase, the loss curve will become very desultory.

The refractive index sensitivity S is an important indicator to measure the performance of the sensor and there are two main approaches for the detection of sensor's sensitivity. One is the wavelength scanning method which can be achieved by using a broadband light source and can be calculated from the following equation:

$$S_\lambda(\lambda)(\mathrm{nm}/RIU) = \partial\lambda_{res}/\partial n_a \tag{2}$$

where λ_{res} refers to the resonance wavelength.

As one can see in Fig. 5 that with the increase of the RI, the coupling wavelength will increase in the form of parabola. A dynamic sensitivity from 3908 nm/RIU to 10694 nm/RIU can be obtained with the corresponding refractive index range from 1.33 to 1.38, which is higher than the value reported in Table 1. A maximum resolution of 9.35×10^{-6} RIU can be obtained by sssuming the spectrometer resolution of $\Delta\lambda = 0.1$ nm.

Alternatively, another simplicity and low cost detection method is the amplitude-(or phase-) based method, where all of the measurements are done at a single wavelength without any spectral manipulations [41] [8]. We assume the transmission loss $\alpha(\lambda, n_a)$ is a function of wavelength and refractive index of analytes, L is the length of the fiber and $P(\lambda, L, n_a)$ is the power launched into the core mode at initial state with RI=n_a of analyte. When the variation of RI is Δ_{n_a}, the amplitude sensitivity can be expressed as:

$$S_A(RIU^{-1}) = \frac{P(\lambda, L, n_a + \Delta_{n_a}) - P(\lambda, L, n_a)}{P(\lambda, L, n_a)\Delta_{n_a}} \tag{3}$$

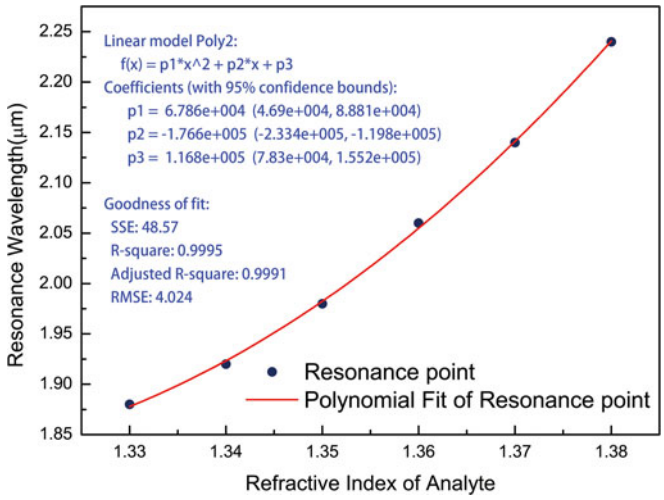

Fig. 5. Numerical fitting result of resonance wavelengths as a function of the refractive index of analyte.

TABLE 1
Performance Comparison of the Reported SPR Sensors

Characteristics	Wavelength(μm)	RI Range	Sensitivity
Graphene based D-shaped fiber [38]	480–650	1.33–1.37	3,700 nm/RIU
hollow-core D-shaped fiber [39]	550–750	1.33–1.34	2,900 nm/RIU
D-shape, single metal coating [40]	750–910	1.35–1.42	5,000 nm/RIU
All-solid D-shaped [17]	N/A	N/A	7300 nm/RIU
Graphene is deposited over a metal layer [26]	1650–1750	1.33–1.345	5700 nm/RIU
Quasi-D-shaped (our work)	1880–2140	1.33–1.38	10694 nm/RIU

When the length of the fiber is defined as $L = \frac{1}{\alpha(\lambda, n_a)}$, the amplitude sensitivity can be reduced to [8]:

$$S_A(\lambda) = \frac{1}{\alpha(\lambda, n_a)} \frac{\partial \alpha(\lambda, n_a)}{\partial n_a} \tag{4}$$

Fig. 6 shows the amplitude sensitivity as a function of RI of analytes. The intensity of SPR increased with the increase of the RI of analyte. Maximum amplitude sensitivity of 95 RIU^{-1} at the wavelength of 2040 nm with the analyte RI 1.37 is obtained and the corresponding sensor resolution is 1.05×10^{-4} by assuming that change in transmission intensity of 1% can be detected.

3.2 Investigating on the Influence of Structural Parameters on the Sensing Performance

As far as we know that the coating material has significant effects on the sensing performance [10] [42]. The coupling between plasmonic mode and the fiber core mode can be greatly affected by the parameters of coating material such as thickness of metal film, layers of graphene sheet, the polishing depth, etc. As can be seen in Fig. 7 that with the number of graphene layers increased from $L = 1$ to $L = 5$ the core mode loss is found to decrease from 59 dB/cm to 51 dB/cm. The

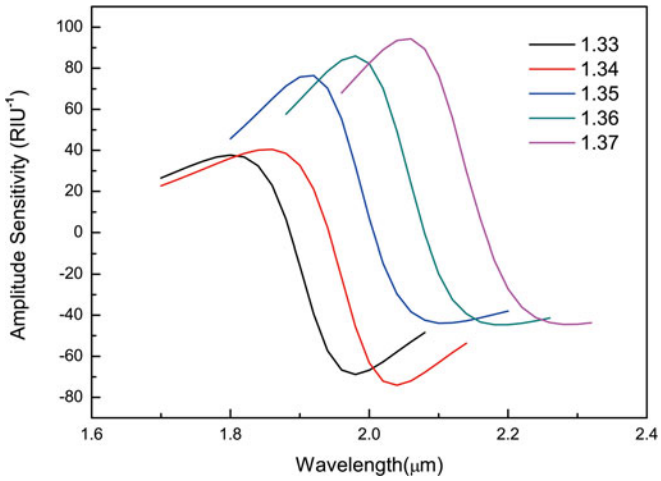

Fig. 6. Amplitude sensitivity variation with different analyte RI 1.33-1.37.

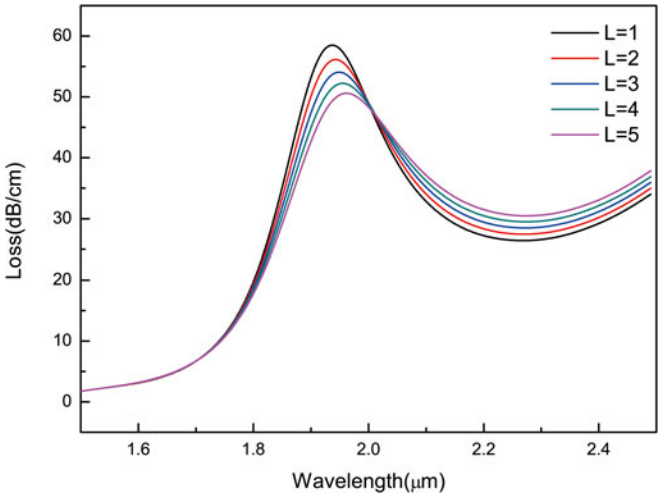

Fig. 7. Variation of loss with different graphene layers.

reason why we considered the maximum number of graphene layers to 5 is that when the number of graphene layers continues to increase the electronic behavior of graphene will be close to bulk graphite according to the infrared conductivity spectra mentioned in Ref [43].

The thickness of the ITO also has a great influence on the sensing performance. With the thickness of the ITO film increased from 90 nm to 120 nm the resonance wavelength experienced a red shift, that is, the loss peak moves to the long-wave direction as is shown in Fig. 8(a). Obviously, changes of metal layer thickness will inevitably lead to the change of sensitivity. We use amplitude sensitivity as an example for all the discussions and illustrations with RI of analyte $n_a = 1.34$. As one can see in Fig. 8(b) that with the increase of the thickness of ITO the maximum amplitude sensitivity has a slight fluctuation ranging from $63RIU^{-1}$ to $68RIU^{-1}$ and the amplitude peak also becomes broader. The maximum amplitude sensitivity leads to sensor resolution of 1.47×10^{-4}.

As can be seen in Fig. 9(a) that with the decrease of polishing depth($3.0\,\mu m - 2.8(93\%)\,\mu m$)-in other words, the sensing medium is becoming more and more away from the fiber core, the loss depth also decrease and experiences a red shift. That is mainly because that with the increase of the distance between the fiber core and the sensing medium, the energy of the core mode is more difficult to couple to the metal surface. The amplitude sensitivity increased a little from $88RIU^{-1}$ to $102RIU^{-1}$ and experienced a red shift at the analyte $RI = 1.35$ which is shown in Fig. 9(b). But the

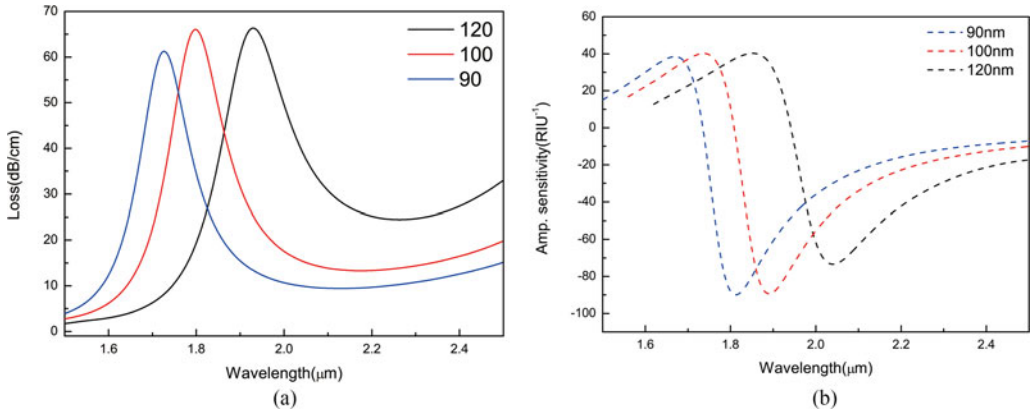

Fig. 8. Effect of ITO thickness on the sensing performance. (a) Variation of loss with different ITO thickness. (b) Amplitude sensitivity effects with varying ITO thickness from 90 nm to120 nm.

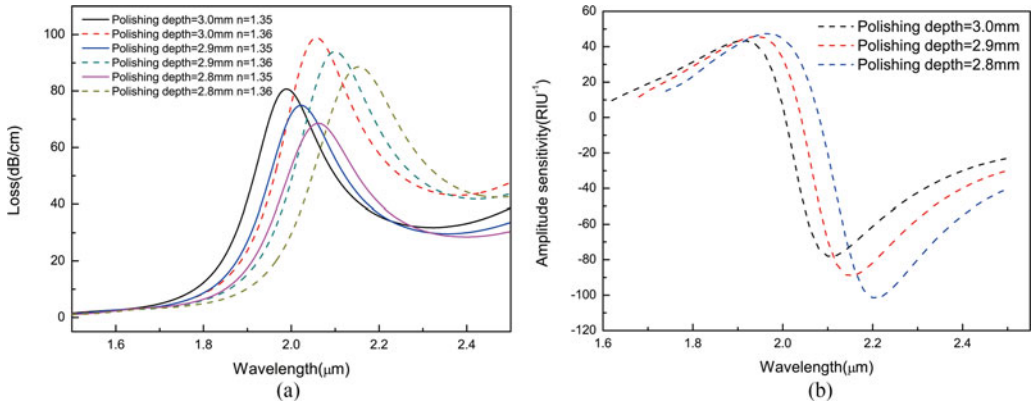

Fig. 9. Variation of loss and amplitude sensitivity with different polishing depths. (a) Variation of loss with different polishing depths. (b) Amplitude sensitivity effects with different polishing depths at analyte RI = 1.35.

polishing depth can not be arbitrarily decreased because that according to our simulation, when the polishing depth reduces to a certain extent the loss depth which used as the test signal will be very small and the detection range of the analyte RI will also be reduced(the loss curve of analyte with high RI (1.37, 1.38, etc.) becomes more desultory and illegible which are very unfavorable for signal detection).

Hence, for the fabrication tolerance, to control the polishing depth within 10% and fine-tuning of the thickness of the metal layer can ensure a good sensing performance of the proposed sensor combines the advantages of quasi-D-shaped structure.

4. Conclusion

A quasi-D-Shaped photonic crystal fiber plasmonic biosensor coated with ITO film and a monolayer of graphene is proposed for refractive index sensing. By placing the core on the edge of the cladding, a shorter polishing depth is achieved so that the production process will be very simple. Also in this way, the impact toughness of the sensor can be greatly enhanced compared to the reported D-shaped fiber sensor. The compute results show that a maximum wavelength interrogation sensitivity of 10693 nm/RIU can be achieved with the corresponding resolution of 9.35×10^{-6} RIU and a maximun amplitude sensitivity of 95 RIU^{-1} with the analyte $RI = 1.37$ is obtained and the corresponding sensor resolution is 1.05×10^{-4}.

References

[1] P. Pattnaik, "Surface plasmon resonance," *Appl. Biochem. Biotechnol.*, vol. 126, no. 2, pp. 79–92, 2005.
[2] S. Zeng, K.-T. Yong, I. Roy, X.-Q. Dinh, X. Yu, and F. Luan, "A review on functionalized gold nanoparticles for biosensing applications," *Plasmonics*, vol. 6, no. 3, 2011, Art. no. 491.
[3] X.-M. Wang, C.-L. Zhao, Y.-R. Wang, C.-Y. Shen, and X.-Y. Dong, "A highly sensitive fibre-optic nano-displacement sensor based on surface plasmon resonance," *J. Lightw. Technol.*, vol. 34, no. 9, pp. 2324–2330, May 2016.
[4] Y. Liu, X. Liu, S. Chen, Q. Liu, and W. Peng, "Investigation of a capillary-based surface plasmon resonance sensor for biosensing," *J. Lightw. Technol.*, vol. 34, no. 17, pp. 4036–4042, Sep. 2016.
[5] L. Wu *et al.*, "Sensitivity improved SPR biosensor based on the mos 2/graphene–aluminum hybrid structure," *J. Lightw. Technol.*, vol. 35, no. 1, pp. 82–87, Jan. 2017.
[6] M. F. O. Hameed, Y. K. Alrayk, A. Shaalan, W. S. El Deeb, and S. Obayya, "Novel multichannel surface plasmon resonance photonic crystal fiber biosensor," *Proc. SPIE*, vol. 9899, 2016, Art. no. 989923.
[7] M. Hautakorpi, M. Mattinen, and H. Ludvigsen, "Surface-plasmon-resonance sensor based on three-hole microstructured optical fiber," *Opt. Express*, vol. 16, no. 12, pp. 8427–8432, 2008.
[8] A. Hassani and M. Skorobogatiy, "Design criteria for microstructured-optical-fiber-based surface-plasmon-resonance sensors," *J. Opt. Soc. Amer. B*, vol. 24, no. 6, pp. 1423–1429, 2007.
[9] B. Gauvreau, A. Hassani, M. F. Fehri, A. Kabashin, and M. Skorobogatiy, "Photonic bandgap fiber-based surface plasmon resonance sensors," *Opt. Express*, vol. 15, no. 18, pp. 11413–11426, 2007.
[10] A. Hassani and M. Skorobogatiy, "Design of the microstructured optical fiber-based surface plasmon resonance sensors with enhanced microfluidics," *Opt. Express*, vol. 14, no. 24, pp. 11616–11621, 2006.
[11] X. Fu, Y. Lu, X. Huang, and J. Yao, "Surface plasmon resonance sensor based on photonic crystal fiber filled with silver nanowires," *Optica Applicata*, vol. 41, no. 4, pp. 941–951, 2011.
[12] W. L. Ng, A. A. Rifat, W. R. Wong, G. Mahdiraji, and F. M. Adikan, "A novel diamond ring fiber-based surface plasmon resonance sensor," *Plasmonics*, pp. 1–6, 2017.
[13] M. R. Hasan, S. Akter, A. A. Rifat, S. Rana, and S. Ali, "A highly sensitive gold-coated photonic crystal fiber biosensor based on surface plasmon resonance," *Photonics*, vol. 4, no. 1., 2017, Art. no. 18.
[14] A. Rifat, G. A. Mahdiraji, Y. Shee, M. J. Shawon, and F. M. Adikan, "A novel photonic crystal fiber biosensor using surface plasmon resonance," *Procedia Eng.*, vol. 140, pp. 1–7, 2016.
[15] Y. Lu, M. Wang, C. Hao, Z. Zhao, and J. Yao, "Temperature sensing using photonic crystal fiber filled with silver nanowires and liquid," *IEEE Photon. J.*, vol. 6, no. 3, Jun. 2014, Art. no. 6801307.
[16] A. A. Rifat, G. Mahdiraji, Y. M. Sua, R. Ahmed, Y. Shee, and F. M. Adikan, "Highly sensitive multi-core flat fiber surface plasmon resonance refractive index sensor," *Opt. Express*, vol. 24, no. 3, pp. 2485–2495, 2016.
[17] M. Tian, P. Lu, L. Chen, C. Lv, and D. Liu, "All-solid D-shaped photonic fiber sensor based on surface plasmon resonance," *Optics Commun.*, vol. 285, no. 6, pp. 1550–1554, 2012.
[18] H.-J. Kim, O.-J. Kown, S. Lee, and Y.-G. Han, "Measurement of temperature and refractive index based on surface long-period gratings deposited onto a d-shaped photonic crystal fiber," *Appl. Phys. B, Lasers Opt.*, vol. 102, no. 1, pp. 81–85, 2011.
[19] Z. Tan, X. Hao, Y. Shao, Y. Chen, X. Li, and P. Fan, "Phase modulation and structural effects in a d-shaped all-solid photonic crystal fiber surface plasmon resonance sensor," *Opt. Express*, vol. 22, no. 12, pp. 15049–15063, 2014.
[20] Y. Ying, G.-y. Si, F.-j. Luan, K. Xu, Y.-w. Qi, and H.-n. Li, "Recent research progress of optical fiber sensors based on d-shaped structure," *Opt. Laser Technol.*, vol. 90, pp. 149–157, 2017.
[21] D. F. Santos, A. Guerreiro, and J. M. Baptista, "SPR microstructured d-type optical fiber sensor configuration for refractive index measurement," *IEEE Sensors J.*, vol. 15, no. 10, pp. 5472–5477, Oct. 2015.
[22] Y. Chen, Q. Xie, X. Li, H. Zhou, X. Hong, and Y. Geng, "Experimental realization of D-shaped photonic crystal fiber SPR sensor," *J. Phys. D, Appl. Phys.*, vol. 50, no. 2, 2016, Art. no. 025101.
[23] F. Liu, S. Li, and X. Guo, "Refractive index sensing characteristics of D-shape double core photonic crystal fiber based on surface plasmon resonance," *Proc. SPIE*, vol. 10155, 2016, Art. no. 101550K.
[24] T. Huang, "Highly sensitive SPR sensor based on D-shaped photonic crystal fiber coated with indium tin oxide at near-infrared wavelength," *Plasmonics*, vol. 12, pp. 583–588, 2017.
[25] D. Hunger, C. Deutsch, R. J. Barbour, R. J. Warburton, and J. Reichel, "Laser micro-fabrication of concave, low-roughness features in silica," *AIP Adv.*, vol. 2, no. 1, 2012, Art. no. 012119.
[26] A. Patnaik, K. Senthilnathan, and R. Jha, "Graphene-based conducting metal oxide coated d-shaped optical fiber spr sensor," *IEEE Photon. Technol. Lett.*, vol. 27, no. 23, pp. 2437–2440, Dec. 2015.
[27] S. K. Mishra and B. D. Gupta, "Surface plasmon resonance-based fiber-optic hydrogen gas sensor utilizing indium–tin oxide (ito) thin films," *Plasmonics*, vol. 7, no. 4, pp. 627–632, 2012.
[28] S. Singh and B. Gupta, "Simulation of a surface plasmon resonance-based fiber-optic sensor for gas sensing in visible range using films of nanocomposites," *Meas. Sci. Technol.*, vol. 21, no. 11, 2010, Art. no. 115202.
[29] O. Salihoglu, S. Balci, and C. Kocabas, "Plasmon-polaritons on graphene-metal surface and their use in biosensors," *Appl. Phys. Lett.*, vol. 100, no. 21, 2012, Art. no. 213110.
[30] J. N. Dash and R. Jha, "Graphene-based birefringent photonic crystal fiber sensor using surface plasmon resonance," *IEEE Photon. Technol. Lett.*, vol. 26, no. 11, pp. 1092–1095, Jun. 2014.
[31] A. A. Rifat *et al.*, "Copper-graphene-based photonic crystal fiber plasmonic biosensor," *IEEE Photon. J.*, vol. 8, no. 1, Feb. 2016, Art. no. 4800408.
[32] S. H. Choi, Y. L. Kim, and K. M. Byun, "Graphene-on-silver substrates for sensitive surface plasmon resonance imaging biosensors," *Opt. Express*, vol. 19, no. 2, pp. 458–466, 2011.
[33] A. A. Rifat, R. Ahmed, G. A. Mahdiraji, and F. M. Adikan, "Highly sensitive d-shaped photonic crystal fiber-based plasmonic biosensor in visible to near-IR," *IEEE Sensors J.*, vol. 17, no. 9, pp. 2776–2783, May 2017.

[34] T. Maruyama and K. Fukui, "Indium tin oxide thin films prepared by chemical vapour deposition," *Thin Solid Films*, vol. 203, no. 2, pp. 297–302, 1991.
[35] J. Zheng and H. S. Kwok, "Low resistivity indium tin oxide films by pulsed laser deposition," *Appl. Phys. Lett.*, vol. 63, no. 1, pp. 1–3, 1993.
[36] M. Ali, K. Ibrahim, O. S. Hamad, M. Eisa, M. Faraj, and F. Azhari, "Deposited indium tin oxide (ito) thin films by dc-magnetron sputtering on polyethylene terephthalate substrate (pet)," *Romanian J. Phys*, vol. 56, nos. 5/6, pp. 730–741, 2011.
[37] D. P. Singh, S. K. Gupta, T. Vimal, and R. Manohar, "Dielectric, electro-optical, and photoluminescence characteristics of ferroelectric liquid crystals on a graphene-coated indium tin oxide substrate," *Phys. Rev. E*, vol. 90, no. 2, 2014, Art. no. 022501.
[38] J. N. Dash and R. Jha, "On the performance of graphene-based D-shaped photonic crystal fibre biosensor using surface plasmon resonance," *Plasmonics*, vol. 10, no. 5, pp. 1123–1131, 2015.
[39] N. Luan, R. Wang, W. Lv, and J. Yao, "Surface plasmon resonance sensor based on D-shaped microstructured optical fiber with hollow core," *Opt. Express*, vol. 23, no. 7, pp. 8576–8582, 2015.
[40] J. Homola, R. Slavík, and J. Čtyrokỳ, "Interaction between fiber modes and surface plasmon waves: Spectral properties," *Opt. Lett.*, vol. 22, no. 18, pp. 1403–1405, 1997.
[41] E. K. Akowuah, G. Robinson, H. Ademgil, J. Oliver, S. Haxha, and T. Gorman, *A novel compact photonic crystal fibre surface plasmon resonance biosensor for an aqueous environment*. Rijeka, Croatia: INTECH Open Access Publisher, 2012.
[42] J. S. Velázquez-González, D. Monzón-Hernández, D. Moreno-Hernández, F. Martínez-Piñón, and I. Hernández-Romano, "Simultaneous measurement of refractive index and temperature using a SPR-based fiber optic sensor," *Sens. Actuators B, Chem.*, vol. 242, pp. 912–920, 2017.
[43] K. F. Mak, M. Y. Sfeir, J. A. Misewich, and T. F. Heinz, "The evolution of electronic structure in few-layer graphene revealed by optical spectroscopy," *Proc. Nat. Acad. Sci. USA*, vol. 107, no. 34, pp. 14999–15004, 2010.